

Electronic Supplementary Information for:

## N-chlorobenzimidazoles as efficient and structurally diverse amphoteric halogen bond donors in crystal engineering

Arun Dhaka,<sup>\*a</sup> Olivier Jeannin,<sup>a</sup> Emmanuel Aubert,<sup>b</sup> Enrique Espinosa,<sup>b</sup> Marc Fourmigué,<sup>a</sup> and Ie-Rang Jeon<sup>\*a</sup>

<sup>a</sup>Univ Rennes, CNRS, ISCR (Institut des Sciences Chimiques de Rennes) UMR 6226, 35042 Rennes, France. E-mail: [ie-rang.jeon@univ-rennes1.fr](mailto:ie-rang.jeon@univ-rennes1.fr)

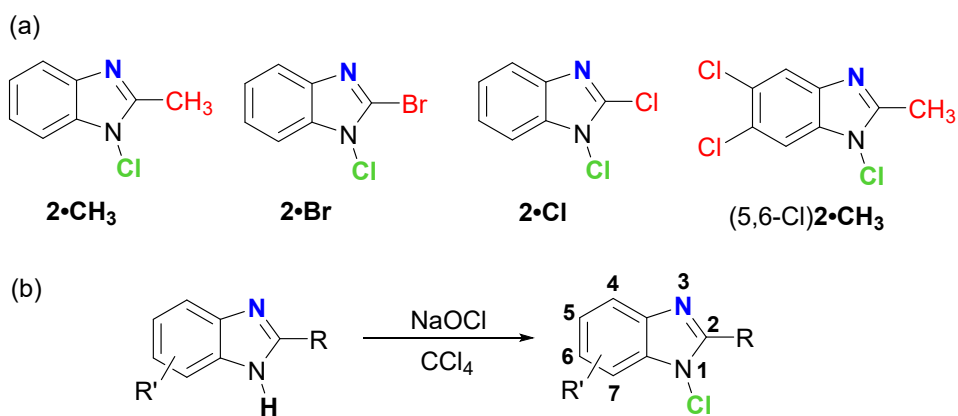
<sup>b</sup>Laboratoire CRM2, UMR CNRS 7036, Institut Jean Barriol, Université de Lorraine, BP 70239, 54506 Vandoeuvre-les-Nancy, France

### Table of contents

<b>A. Synthetic procedures</b>	page 2
<b>B. NMR Spectra</b>	page 3
<b>C. Crystallography and Table S1</b>	page 7
<b>Figure S1</b> ESP maps of <b>2•CH<sub>3</sub></b> , <b>2•Br</b> , <b>2•Cl</b> , and (5,6-Cl) <b>2•CH<sub>3</sub></b>	page 8
<b>Figure S2</b> Details of secondary intermolecular interactions in <b>2•CH<sub>3</sub></b>	page 8
<b>D. Theoretical calculations and Table S2</b>	page 9
<b>Figure S3</b> ESP maps of <b>2•CH<sub>3</sub></b> , <b>2•Br</b> , <b>2•Cl</b> , and (5,6-Cl) <b>2•CH<sub>3</sub></b>	page 9
<b>Table S2</b> Calculated electrostatic potential values at selected molecular sites	page 10
<b>Figure S4.</b> Optimized n = 6 chain extracted from the crystal structure of <b>2•Cl</b>	page 10
<b>Table S3.</b> Electrostatic and geometrical properties in <b>2•Cl</b> with increasing chain length	page 10
<b>Figure S5</b> Optimized n= 5 chains in pair extracted from the crystal structure of <b>2•Cl</b>	page 11
<b>Table S4.</b> Electrostatic and geometrical properties of <b>2•Cl</b> chains in pair with increasing chain length	page 11
<b>References</b>	page 12

## A. Synthetic procedures

**General considerations:** Oxygen- and moisture-sensitive experiments were carried out under a dry oxygen-free nitrogen atmosphere using standard Schlenk techniques. Solvents were dried by standard methods. The NMR spectra were recorded on Bruker spectrometers (300 MHz) referenced to residual solvent signals as internal standards. Elemental analyses were performed at BioCIS (Elementar Vario/Perkin Elmer 2400 series). Commercially available benzimidazole derivatives **2•CH<sub>3</sub>**, **2•Br**, **2•Cl**, (5,6-Cl)**2•CH<sub>3</sub>** and 14% sodiumhypochlorite (NaOCl) solution were purchased and used as received (Scheme S1).



**Scheme S1** a) N-chlorobenzimidazoles derivatives synthesized in this study b) synthesis strategy.

**General synthetic procedure:** The appropriate N-(H)benzimidazole (300 mg), was suspended in CCl<sub>4</sub> (30 mL) and added NaOCl (13–15% solution) in excess (10 ml). Reaction was stirred for 4–5 hours to obtain a clear solution. Organic layer was washed with water and extracted using CCl<sub>4</sub> as a solvent. The combined organic layers were concentrated under vacuum using rotary evaporator to obtain a white solid in moderate yields 30–60%. The obtained solid was recrystallized from ethyl acetate solution to afford colourless crystals.

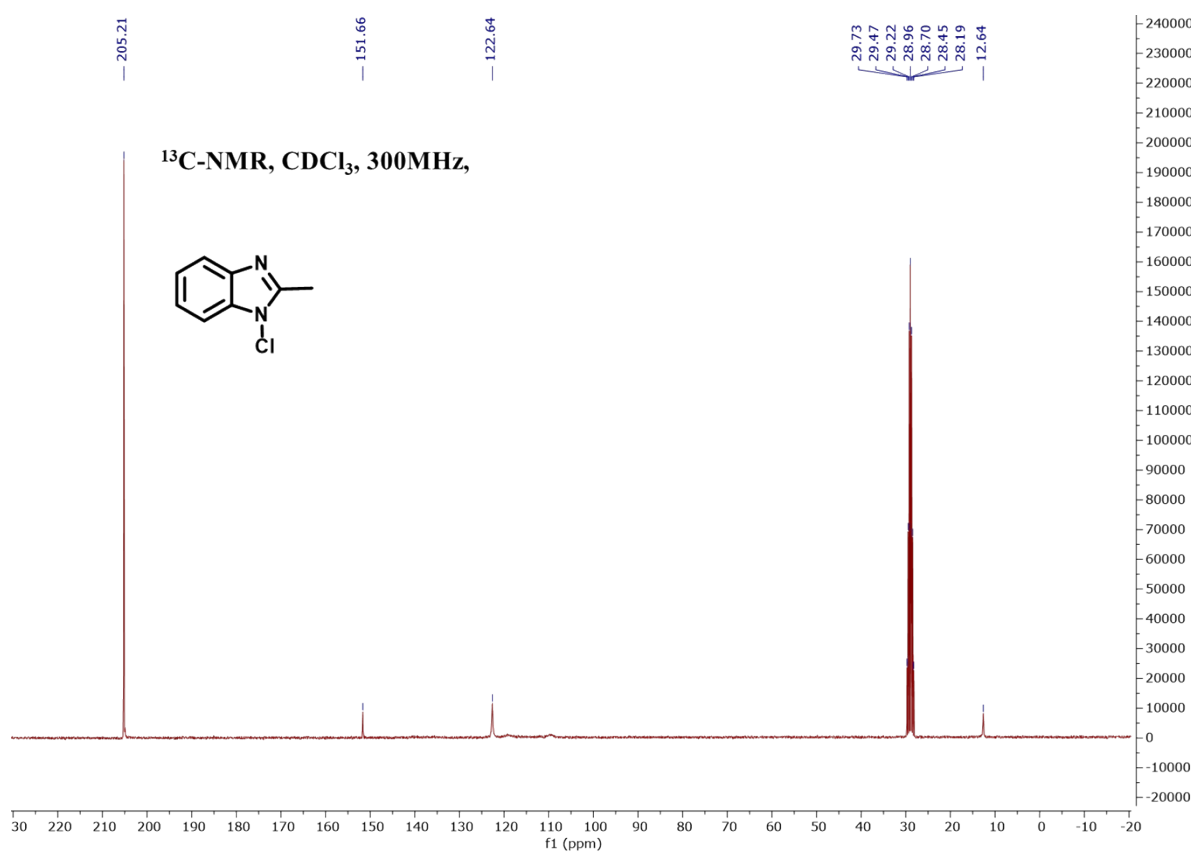
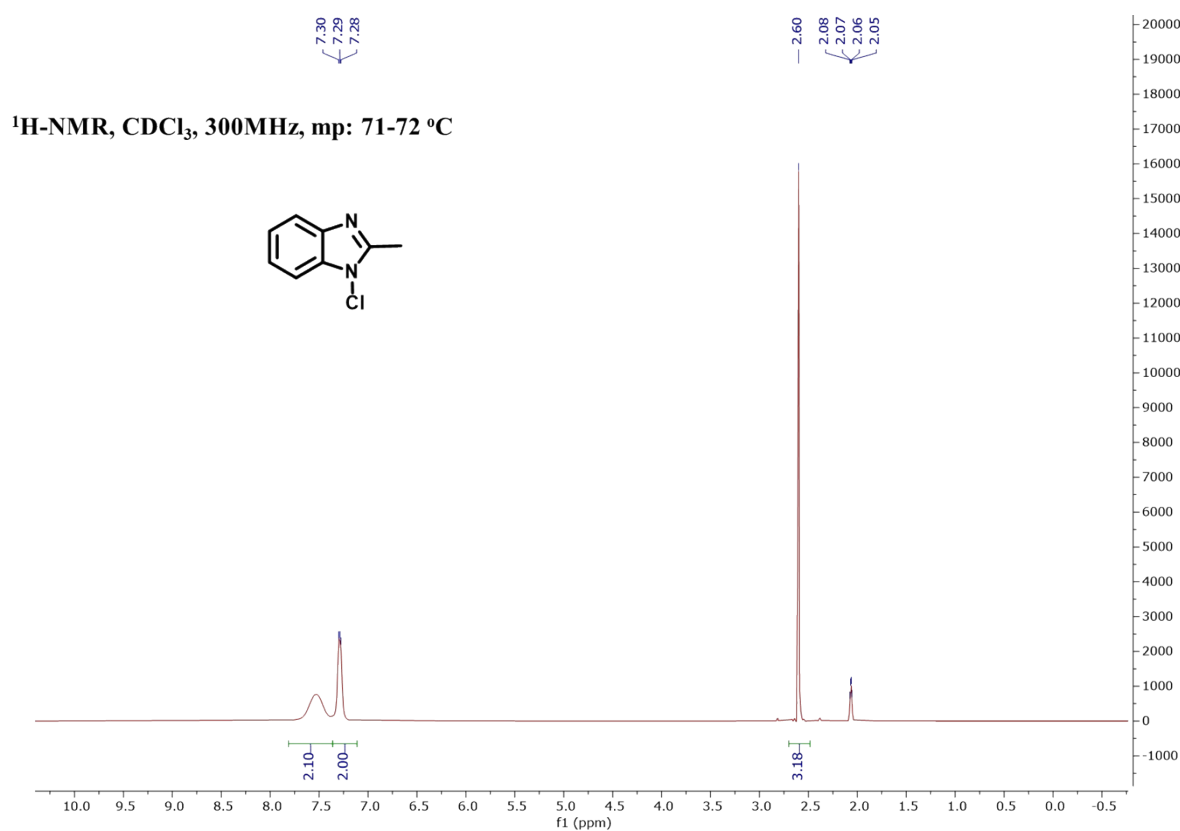
**2•CH<sub>3</sub>:** <sup>1</sup>H NMR (300 MHz, Acetone-D6) δ 7.72–7.61 (m, 1H), 7.44–7.41 (m, 1H), 7.37–7.28 (m, 2H), 2.68 (s, 3H). <sup>13</sup>C NMR (300 MHz, Acetone-D6) δ 12.7, 122.6, 151.7, 205.2. Mp: 71–72°C. Anal. Calcd. for C<sub>8</sub>H<sub>7</sub>N<sub>2</sub>Cl: C, 57.67; H, 4.23; N, 16.81. Found: C, 58.39; H, 4.19; N, 16.97.

**2•Br:** <sup>1</sup>H NMR (300 MHz, Acetone-D6) δ 7.70–7.67 (m, 1H), 7.57–7.53 (m, 1H), 7.46–7.41 (m, 1H), 7.38–7.32 (m, 1H). <sup>13</sup>C NMR (300 MHz, Acetone-D6) δ 109.9, 119.7, 123.5, 124.6. Mp: 67–68°C. Anal. Calcd. for C<sub>7</sub>H<sub>4</sub>N<sub>2</sub>ClBr: C, 36.32; H, 1.74; N, 12.10. Found: C, 36.15; H, 1.65; N, 11.76.

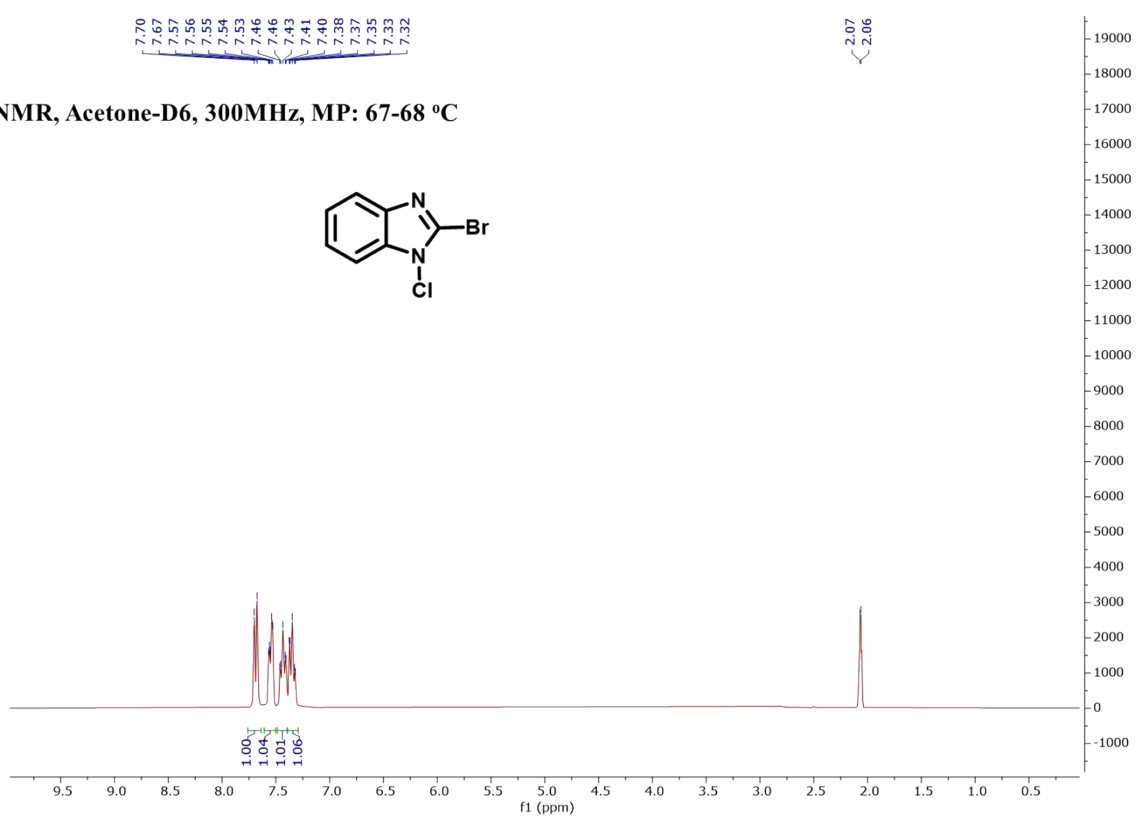
**2•Cl:** <sup>1</sup>H NMR (300 MHz, Acetone-D6) δ 7.69–7.66 (m, 1H), 7.56–7.52 (m, 1H), 7.48–7.43 (m, 1H), 7.40–7.35 (m, 1H). <sup>13</sup>C NMR (300 MHz, Acetone-D6) δ 109.9, 119.8, 123.7, 124.7. Mp: 64–65°C. Anal. Calcd. for C<sub>7</sub>H<sub>4</sub>N<sub>2</sub>Cl<sub>2</sub>: C, 44.95; H, 2.16; N, 14.98. Found: C, 45.22; H, 2.12; N, 14.53.

**(5,6-Cl)2•CH<sub>3</sub>:** <sup>1</sup>H NMR (300 MHz, CDCl<sub>3</sub>) δ 7.78 (s, 1H), 7.58 (s, 1H) 2.66 (s, 3H). <sup>13</sup>C NMR (300 MHz, CDCl<sub>3</sub>) δ 110.8, 121.1, 127.3, 127.8, 134.6, 139.9, 153.85. Mp: 155°C. Anal. Calcd. for C<sub>8</sub>H<sub>5</sub>N<sub>2</sub>Cl<sub>3</sub>: C, 40.80; H, 2.14; N, 11.90. Found: C, 40.79; H, 2.04; N, 11.64.

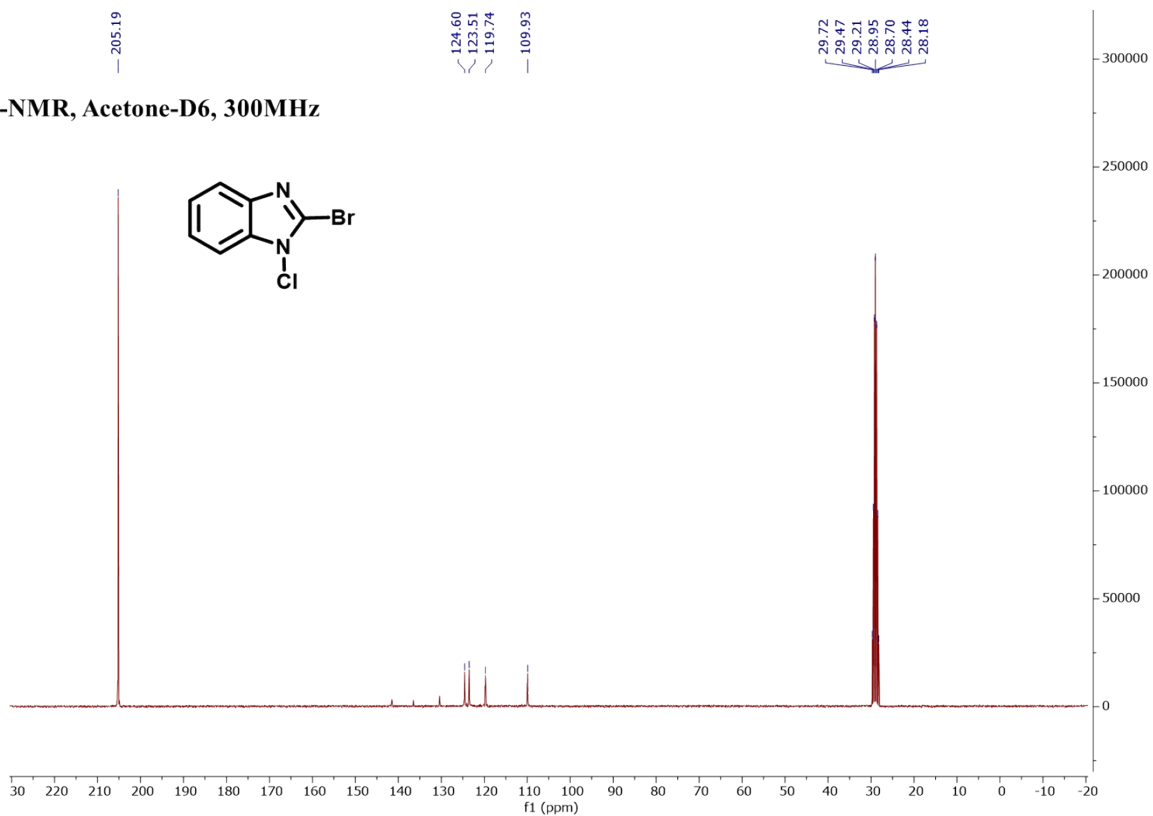
## B. NMR Spectra

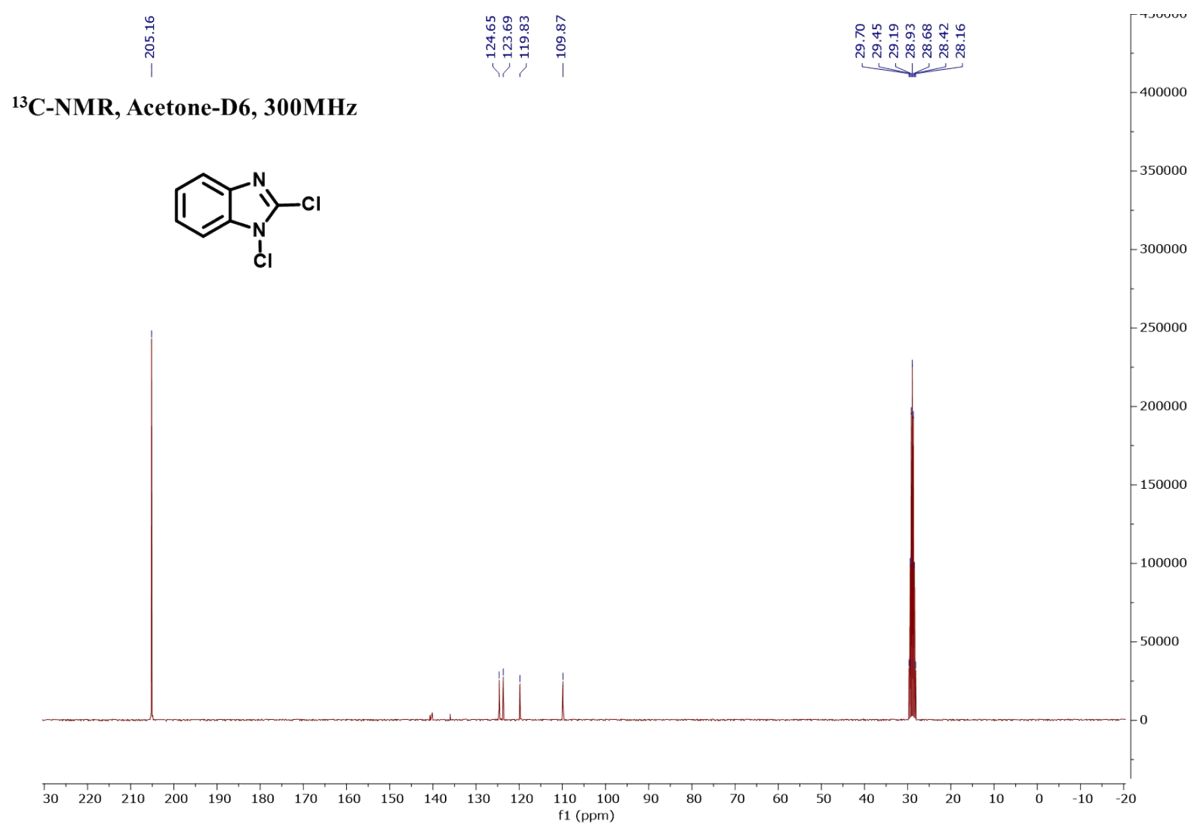
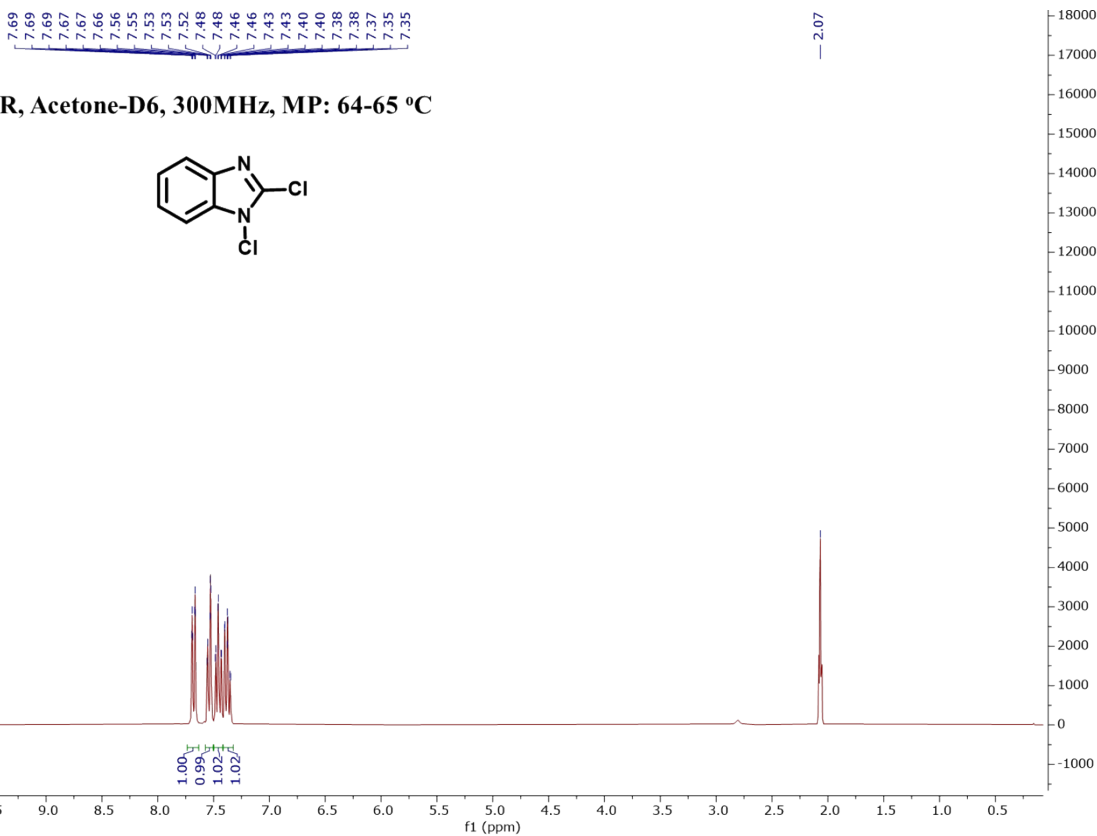


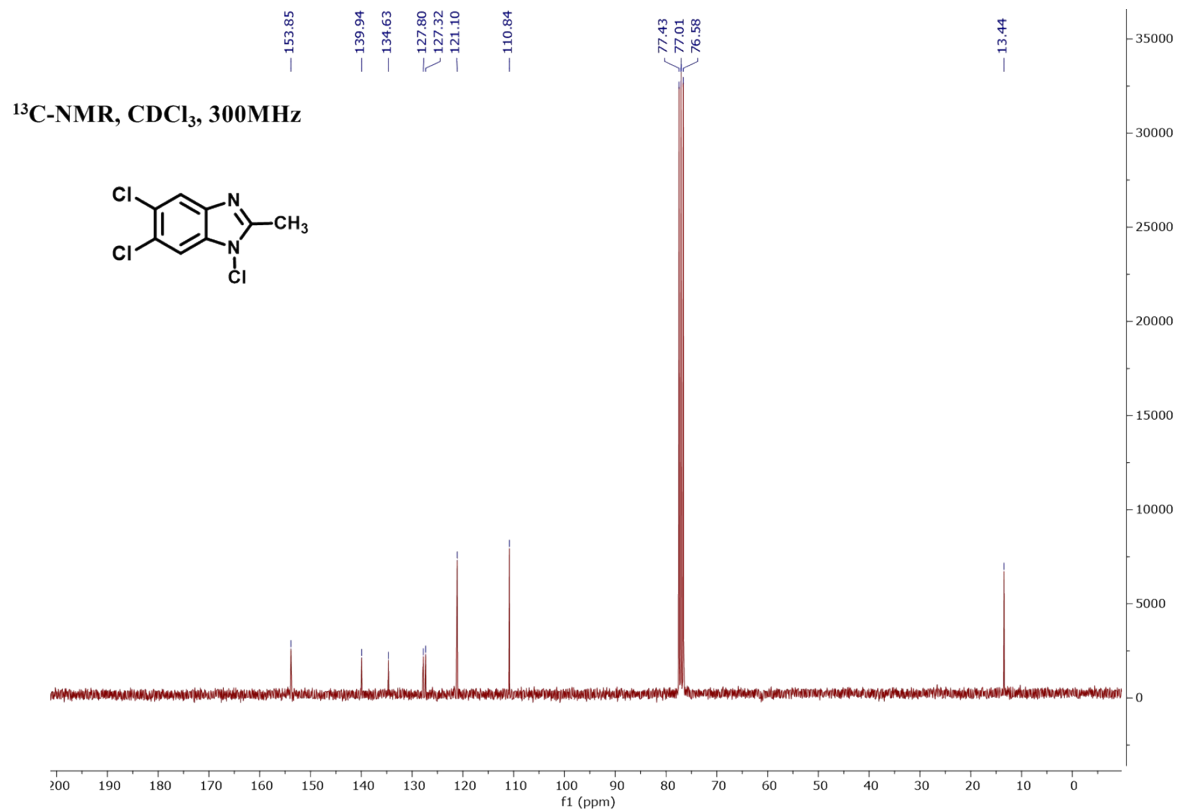
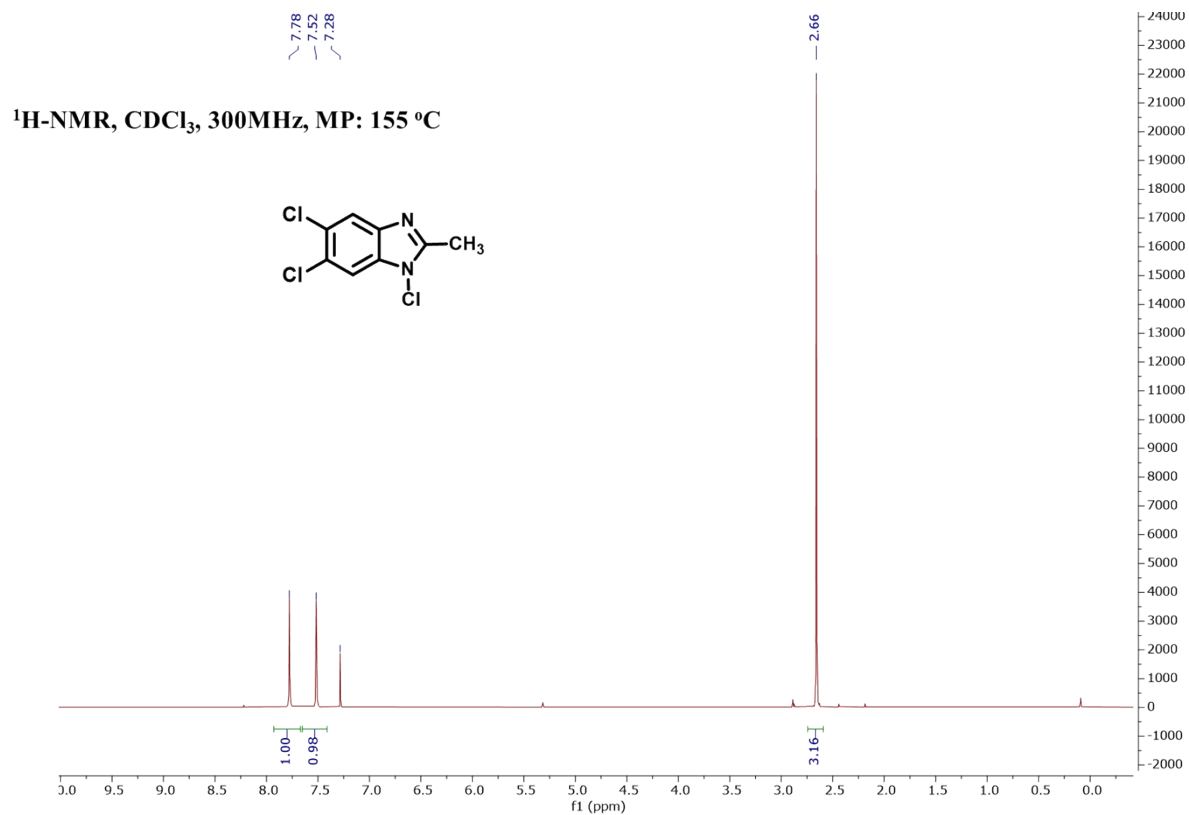
<sup>1</sup>H-NMR, Acetone-D6, 300MHz, MP: 67-68 °C



<sup>13</sup>C-NMR, Acetone-D6, 300MHz







**C. Crystallography:** Details about data collection and solution refinement are given in Table S1. Data collections were performed at ambient temperature on an APEXII Bruker-AXS diffractometer equipped with a CCD camera for all compounds. Structures were solved by direct methods using the *SIR97* program<sup>1</sup> or by dual-space algorithm using *SHELXT*<sup>2</sup> and then refined with full-matrix least-square methods based on *F*<sup>2</sup> (*SHELXL-2014*)<sup>3</sup> with the aid of the *WINGX* program.<sup>4</sup> All non-hydrogen atoms were refined with anisotropic atomic displacement parameters. H atoms were finally included in their calculated positions. Crystallography data (in cif format) have been deposited with deposition numbers CCDC 2173224–2173227.

**Table S1** Crystallographic data

Compound	<b>2•CH<sub>3</sub> (AD46)</b>	<b>2•Br (AD66)</b>	<b>2•Cl (AD65)</b>	<b>(5,6-Cl)2•CH<sub>3</sub></b>
Formulae	C <sub>8</sub> H <sub>7</sub> CIN <sub>2</sub>	C <sub>7</sub> H <sub>4</sub> BrClN <sub>2</sub>	C <sub>7</sub> H <sub>4</sub> Cl <sub>2</sub> N <sub>2</sub>	C <sub>8</sub> H <sub>5</sub> Cl <sub>3</sub> N <sub>2</sub>
FW (g.mol <sup>-1</sup> )	166.61	231.48	187.02	235.49
System	monoclinic	orthorhombic	monoclinic	monoclinic
Space group	P2 <sub>1</sub> /c	Pcab	P2 <sub>1</sub> /n	P2 <sub>1</sub> /c
a (Å)	8.0888(5)	9.3593(11)	7.9412(15)	3.9218(4)
b (Å)	12.0248(7)	12.3411(18)	9.2207(16)	12.4195(11)
c (Å)	8.8930(5)	13.8369(19)	10.7738(15)	18.9195(16)
α (deg)	90	90	90	90
β (deg)	110.940(3)	90	98.837(9)	94.528(3)
γ (deg)	90	90	90	90
V (Å <sup>3</sup> )	807.86(8)	1598.2(4)	779.5(2)	918.63(15)
T (K)	296(2)	296(2)	296(2)	296(2)
Z	4	8	4	4
Cryst. dim. (mm)	0.26×0.11×0.07	0.15×0.12×0.04	0.18×0.09×0.03	0.24×0.11×0.05
D <sub>calc</sub> (g.cm <sup>-1</sup> )	1.370	1.924	1.594	1.703
μ (mm <sup>-1</sup> )	0.403	5.406	0.759	0.944
Total refls	6626	6487	4738	19525
Abs. corr.	multi scan	multi scan	multi scan	multi scan
T <sub>min</sub> , T <sub>max</sub>	0.948, 0.972	0.464, 0.806	0.921, 0.977	0.883, 0.954
Uniq refls (R <sub>int</sub> )	1853 (0.0242)	13910 (0.0661)	1745 (0.0291)	2099 (0.0388)
Uniq refls (I > 2σ(I))	1427	1085	1147	1740
R <sub>1</sub> , wR <sub>2</sub> (I > 2σ(I))	0.0358, 0.0901	0.0470, 0.0728	0.0403, 0.0788	0.0354, 0.0787
R <sub>1</sub> , wR <sub>2</sub> (all data)	0.0529, 0.1022	0.1036, 0.0851	0.0790, 0.0935	0.0477, 0.8445
GOF	1.023	1.0983	1.043	1.059
Res. dens. (e <sup>-</sup> /Å <sup>3</sup> )	0.207, -0.213	0.542, -0.540	0.267, -0.205	0.274, -0.232

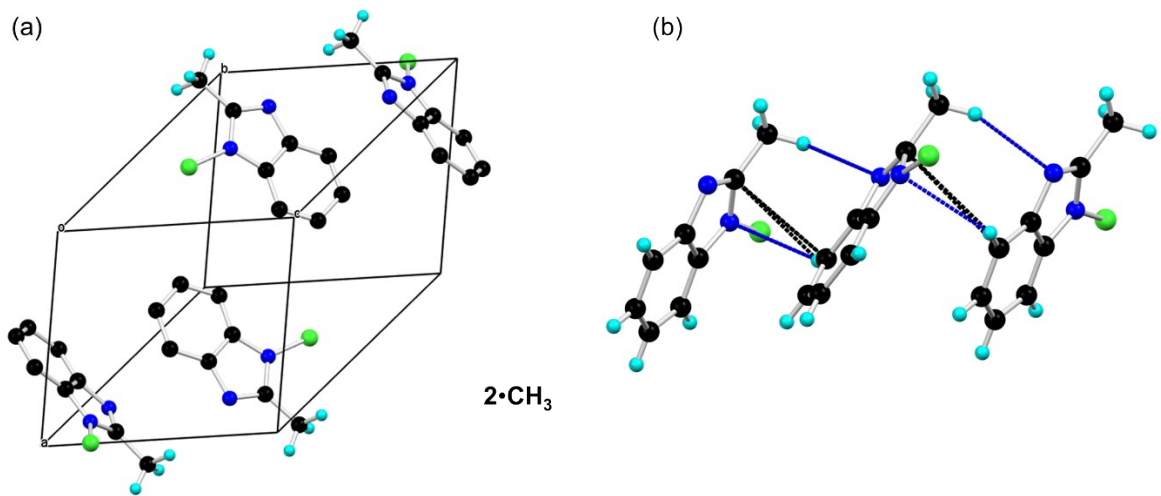


**Figure S1.** a) Molecular positioning in the unit cell of **2·CH<sub>3</sub>** b) C-H $\cdots$ N (blue) and  $\pi\cdots\pi$  (black) interactions between the molecular chains.

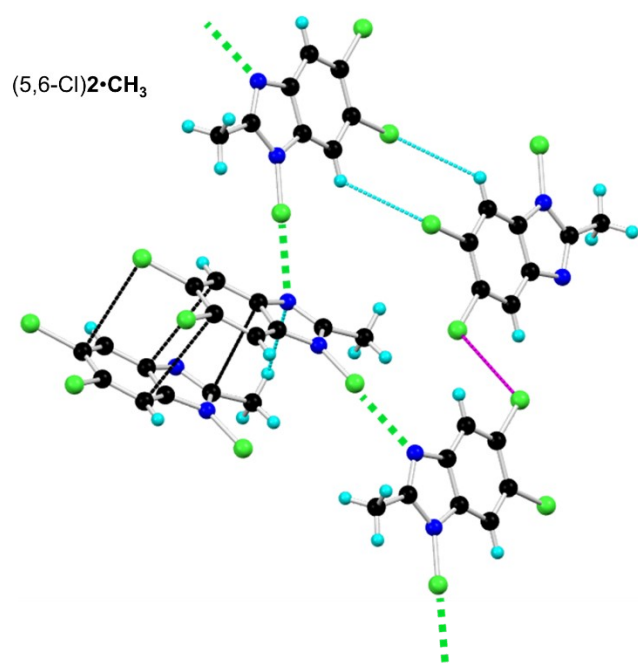


**Figure S2.** Secondary intermolecular interactions in **(5,6-Cl)2·CH<sub>3</sub>** i.e. type I Cl $\cdots$ Cl (pink), Cl/N $\cdots$ H (light blue) and  $\pi\cdots\pi$  (black) interactions between the molecular chains.

#### D. Theoretical calculations

Molecular structures of the four XB based amphoteric system ( $\text{2}\bullet\text{CH}_3$ ,  $\text{2}\bullet\text{Br}$   $\text{2}\bullet\text{Cl}$  and  $\text{2}\bullet\text{CH}_3$ ) have been optimized in gas phase (vacuum) with Gaussian09 software<sup>5</sup> using Density Functional Theory. B3LYP functional was used, completed with D3 dispersion Grimme dispersion correction.<sup>6</sup> The Def2TZVPP basis set was employed for all atoms.<sup>7</sup> Frequency calculations were performed in order to check that true energy minima were obtained. Isosurfaces of electron density ( $\rho = 0.001$  a.u.) mapped with the corresponding total electrostatic potential were calculated and drawn with AIMAll software.<sup>8</sup> Extrema of the electrostatic potential were located with MWFN software.<sup>9</sup>

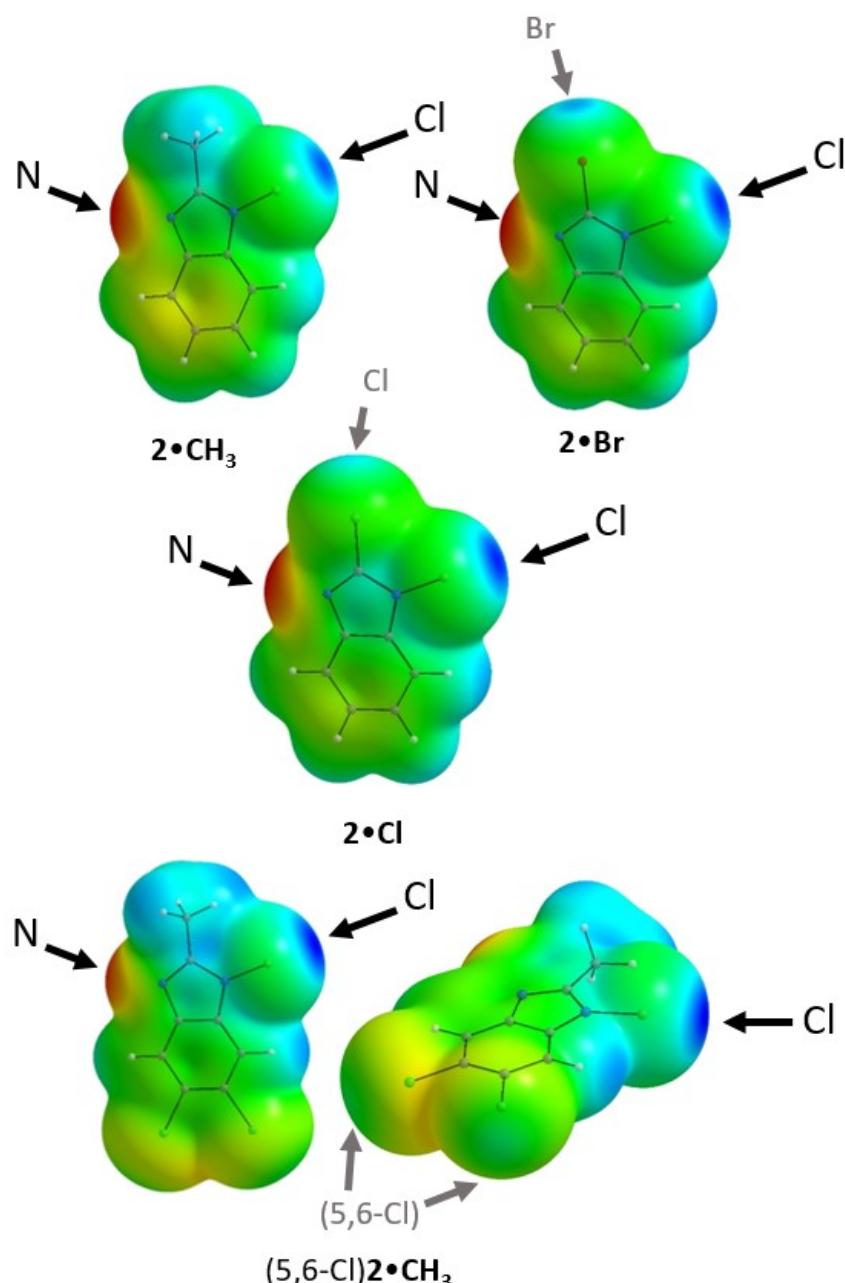


**Figure S3.** Electrostatic potential mapped on the 0.001 a.u. electron density isosurface. Color range: -0.05 a.u. (red) to +0.05 a.u. (blue). Principal donor (Cl) and acceptor (N) sigma-hole interactions sites are shown with black arrows, whereas secondary sites (Cl, Br) are shown in grey.

**Table S2** Calculated electrostatic potential values at selected molecular sites and experimentally observed Cl $\bullet\bullet\bullet$  N<sub>A</sub> and N<sub>D</sub>-Cl distances.

Compound	V <sub>S,max</sub> (N1-Cl) (kcal/mol)	V <sub>S,min</sub> (N <sub>A</sub> ) (kcal/mol)	V <sub>S,max</sub> (C2-Cl,Br) (kcal/mol)	V <sub>S,max</sub> (C5-Cl) (kcal/mol))	V <sub>S,max</sub> (C6-Cl) (kcal/mol))	Cl $\bullet\bullet\bullet$ N <sub>A</sub> (Å)	N <sub>D</sub> -Cl (Å)
<b>2•CH<sub>3</sub></b>	+26.41	-35.39	/	/	/	2.648(2)	1.692(1)
<b>2•Br</b>	+29.19	-33.23	+20.70	/	/	2.652(4)	1.694(4)
<b>2•Cl</b>	+29.42	-33.42	+15.77	/	/	2.695(2)	1.689(2)
(5,6-Cl) <b>2•CH<sub>3</sub></b>	+31.27	-30.08	/	+4.78	+6.42	2.771(2)	1.697(2)

Cooperativity effects were examined in the case of the crystal structure of **2•Cl**. A chain formed by N<sub>D</sub>-Cl $\bullet\bullet\bullet$  N<sub>A</sub> interactions of increasing length was considered, keeping all aromatic carbons fixed at their experimental position while optimizing all the other atoms (same calculation conditions than in previous isolated molecule computations). The V<sub>S,max</sub> (N1-Cl) values are gathered in Table S3, as a function of the chain length, showing a gradual increase and therefore proving a cooperative effect along the chain.

A second type of molecular chains formed by N<sub>D</sub>-Cl $\bullet\bullet\bullet$  N<sub>A</sub> interactions was considered, here taking into account also the most stabilizing  $\pi\cdots\pi$  stacking interactions formed around crystallographic inversion centres (Fig S5, Table S4). In this case, a cooperative effect also displays. Thus, longer chains induce deeper electropositive  $\sigma$ -holes on terminal Cl atoms, although the amplitude of the effect is reduced in comparison to the simple chain.

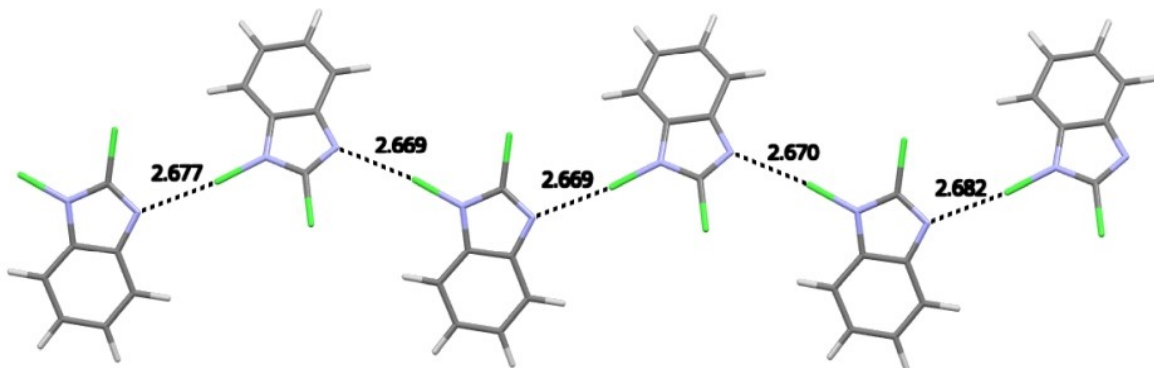


**Figure S4.** Optimized n=6 chain extracted from the crystal structure of **2•Cl** (aromatic C-atoms frozen).

**Table S3.** Electrostatic (V<sub>S,max</sub>) and geometrical properties (interatomic distances, Å) in **2•Cl** for N<sub>D</sub>-Cl $\bullet\bullet\bullet$  N<sub>A</sub> chains of increasing length (*n* being the number of molecules in the chain)

		1	1...2	2	2...3	3	3...4	4	4...5	5	5...6	6
<i>n</i>	V <sub>S,max,Cl</sub> (kcal/mol)	Cl-N	N...Cl	Cl-N								
1	29.22	1.688										
2	34.17	1.688	2.690	1.700								
3	36.16	1.687	2.680	1.701	2.685	1.702						
4	37.17	1.688	2.677	1.701	2.673	1.703	2.683	1.702				
5	37.76	1.688	2.677	1.702	2.670	1.705	2.671	1.704	2.683	1.702		
6	38.15	1.688	2.677	1.702	2.669	1.705	2.669	1.705	2.670	1.705	2.682	1.703

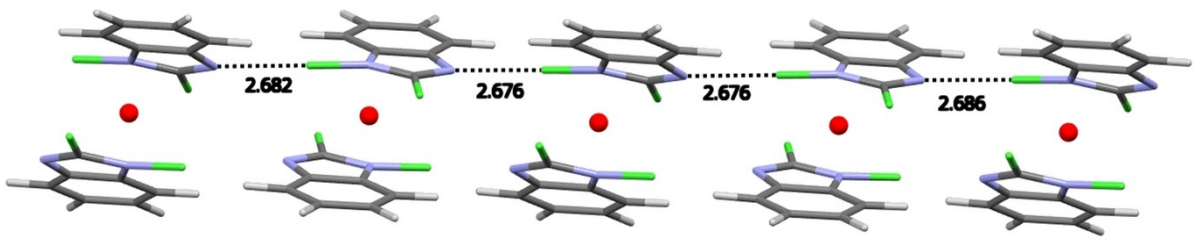


**Figure S5** Optimized  $n = 5$  chain extracted from the crystal structure of **2•Cl** (aromatic C-atoms frozen), considering pairs of symmetry related molecules by crystallographic inversion centres displayed as red spheres.

**Table S4.** Electrostatic ( $V_{s,\max}$ ) and geometrical properties (interatomic distances, Å) in **2•Cl** for  $N_D$ - $Cl \bullet \bullet N_A$  double chains of increasing length ( $n$  being the number of molecules in the chain)

		1	1...2	2	2...3	3	3...4	4	4...5	5
$n$	$V_{s,\max}, Cl$	Cl-N	N...Cl	Cl-N	N...Cl	Cl-N	N...Cl	Cl-N	N...Cl	Cl-N
1	27.84	1.688								
2	30.93	1.687	2.692	1.700						
3	32.04	1.686	2.684	1.700	2.686	1.701				
4	32.62	1.687	2.682	1.701	2.676	1.703	2.685	1.702		
5	32.94	1.686	2.682	1.701	2.676	1.704	2.676	1.704	2.686	1.702

## References

- 1) A. Altomare, M. C. Burla, M. Camalli, G. Cascarano, C. Giacovazzo, A. Guagliardi, A. G. G. Moliterni, G. Polidori and R. Spagna, *J. Appl. Cryst.*, 1999, **32**, 115–119.
- 2) G. M. Sheldrick, *Acta Cryst.* 2015, **A71**, 3–8
- 3) G. M. Sheldrick, *Acta Cryst.* 2015, **C71**, 3–8.
- 4) L. J. Farrugia, *J. Appl. Cryst.*, 2012, **45**, 849–854.
- 5) M. J. Frisch, G. W. Trucks, H. B. Schlegel, G. E. Scuseria, M. A. Robb, J. R. Cheeseman, G. Scalmani, V. Barone, B. Mennucci, G. A. Petersson, H. Nakatsuji, M. Caricato, X. Li, H. P. Hratchian, A. F. Izmaylov, J. Bloino, G. Zheng, J. L. Sonnenberg, M. Hada, M. Ehara, K. Toyota, R. Fukuda, J. Hasegawa, M. Ishida, T. Nakajima, Y. Honda, O. Kitao, H. Nakai, T. Vreven, J. A. Montgomery, Jr., J. E. Peralta, F. Ogliaro, M. Bearpark, J. J. Heyd, E. Brothers, K. N. Kudin, V. N. Staroverov, R. Kobayashi, J. Normand, K. Raghavachari, A. Rendell, J. C. Burant, S. S. Iyengar, J. Tomasi, M. Cossi, N. Rega, J. M. Millam, M. Klene, J. E. Knox, J. B. Cross, V. Bakken, C. Adamo, J. Jaramillo, R. Gomperts, R. E. Stratmann, O. Yazyev, A. J. Austin, R. Cammi, C. Pomelli, J. W. Ochterski, R. L. Martin, K. Morokuma, V. G. Zakrzewski, G. A. Voth, P. Salvador, J. J. Dannenberg, S. Dapprich, A. D. Daniels, Ö. Farkas, J. B. Foresman, J. V. Ortiz, J. Cioslowski, and D. J. Fox, Gaussian 09 (Gaussian, Inc., Wallingford CT, 2009).
- 6) S. Grimme, J. Antony, S. Ehrlich and H. Krieg, *J. Chem. Phys.*, 2010, **132**, 154104.
- 7) F. Weigend and R. Ahlrichs. *Phys. Chem. Chem. Phys.* 2005, **7** 3297-305.
- 8) AIMAll (Version 19.10.12), T. A. Keith, TK Gristmill Software, Overland Park KS, USA, 2019 ([aim.tkgristmill.com](http://aim.tkgristmill.com)).
- 9) T. Lu, F. Chen, *J. Mol. Graph. Model.*, 2012, **38**, 314–323.